Enhanced ferromagnetism in CuO nanowires on the top of CuO nanograins

J. A. Souza, D. Criado, A. Zuniga, V. N. Miranda, F. E. N. Ramirez et al.

Citation: J. Appl. Phys. **114**, 173907 (2013); doi: 10.1063/1.4829284
View online: http://dx.doi.org/10.1063/1.4829284
View Table of Contents: http://jap.aip.org/resource/1/JAPIAU/v114/i17
Published by the AIP Publishing LLC.

Enhanced ferromagnetism in CuO nanowires on the top of CuO nanograins

J. A. Souza,[1,a)] D. Criado,[1] A. Zuniga,[1] V. N. Miranda,[1] F. E. N. Ramirez,[1] S. H. Masunaga,[2] and R. F. Jardim[2]
[1]*Universidade Federal do ABC, Santo André, SP, Brazil*
[2]*Instituto de Física, Universidade de São Paulo, CP 66318, 05315-970 São Paulo, SP, Brazil*

(Received 2 July 2013; accepted 22 October 2013; published online 5 November 2013)

CuO nanograins (NGs) and CuO nanowires (NWs) on the top of nanograins samples were produced by the electrical resistive heating method. The NGs sample shows absence of long range magnetic order and strong field-induced ferromagnetic behavior. In the sample comprised of NWs on the top of NGs, a long-ranged antiferromagnetic ordering is induced by a magnetic field of 5 kOe and coexists with an enhanced ferromagnetic-like contribution. The ferromagnetic behavior is observed below and above the temperature-induced T_N suggesting that this behavior is not dependent on the original magnetic state of the system, whether it is paramagnetic (PM) or antiferromagnetic. © *2013 AIP Publishing LLC*. [http://dx.doi.org/10.1063/1.4829284]

In the past few years, a considerable effort has been devoted in order to grow magnetoelectric nanostructured materials. Besides being of great importance to fundamental science, they are very attractive in the electronic industry, magnetic storage media, and solar energy conversion.[1] Semiconducting along with ferromagnetic (FM) properties have also attracted great attention from the material science community due to not only fundamental science but also technological application. Ferromagnetism at room temperature in the absence of any magnetic doping has been observed in many oxides and in thin films with semiconducting and diamagnetic properties.[2] In this sense, careful experiments must be performed in order to avoid impurity and contamination.[3] As far as this point is concerned, it is believed that all metal oxides (even those with zero effective magnetic moment in nanostructured form) would exhibit ferromagnetic-like properties at room temperature which is absent in bulk samples.[4] The size and shape of the nanostructures are important parameters related to the occurrence or not of this kind of ferromagnetism. The general understanding is that the origin of ferromagnetism in these materials is the magnetic exchange interactions between localized electron spin moments resulting from uncompensated charges and/or intrinsic defects.

Among metal oxides, CuO occupies a special place in the semiconducting *3d* systems due to its unique physical properties.[5] It is believed that CuO is a magnetoelectric system where a ferroelectric order is induced by the onset of a magnetic coupling at low temperatures.[6] More recently, other works have shown that the morphology of CuO nanostructured materials plays an important role in the gas sensing performance.[7,8] Within this context, the characterization of nanostructures unraveling the coexisting magnetic contributions assumes fundamental importance for those applications. In this work, we report the structural, morphological, and magnetization characterizations obtained on nanostructured samples of CuO produced by the electrical resistive thermal method. We have observed that CuO nanograins (NGs) sample shows absence of magnetic ordering, but a magnetic field-induced ferromagnetic behavior shows up in the entire studied temperature range. The samples of CuO nanowires (NWs) on NGs show a temperature-induced bulk like antiferromagnetic (AFM) ordering only when magnetic fields of 5 kOe are applied. A robust FM contribution was observed to coexist with AFM ordering.

X-ray powder diffraction (XRD) data were collected at room temperature on a D8 Discover diffractometer. Scanning electron microscopy (SEM) images were obtained using a JEOL FEG-SEM in the UFABC multiuser facility, while Transmission Electron Microscopy (TEM) images were obtained using a JEOL 2100F FEG-TEM operated at 200 kV in the Brazilian Nanotechnology National Laboratory, Campinas. Magnetization measurements were performed in a superconducting quantum interference device (SQUID) magnetometer.

The synthesis of CuO nanowires was carried out in ambient laboratory conditions by the electrical resistive heating method.[9] The as-received pure copper metal wire (99.9%) of 0.5 mm in diameter and 150 mm in length, suspended between two electric contacts, was heated by the application of a direct electric current. After this process, the oxidized copper in a layered structure released from the metal core. Fig. 1 shows a SEM image of nanostructured oxidized copper produced by the application of an electrical current of 15 A. The image reveals the formation of few nanosheets that coexist with NGs of CuO. It is worth mentioning that underneath the CuO NGs there is a thick Cu_2O layer. X-ray powder diffraction measurements along with Rietveld refinement indicate the presence of two crystal phases: CuO and Cu_2O. The analysis also indicates that Cu_2O is the dominant phase with a cubic structure, space group *Pn-3m*, and that CuO nanostructures crystallize in a monoclinic setting—space group *C2/c*. The main Cu_2O phase reaches a volume fraction close to 86% and the CuO phase ~14%. The unit cell parameters in agreement with literature[10] are: $a = 4.2584(1)$ Å and $V = 77.22(1)$ Å^3 for Cu_2O and $a = 4.667(3)$ Å, $b = 3.419(2)$ Å, $c = 5.114(4)$ Å, $\beta = 99.38(2)^\circ$, and $V = 80.53(3)$ Å^3 for CuO.

a)Author to whom correspondence should be addressed. Electronic mail: joseantonio.souza@ufabc.edu.br

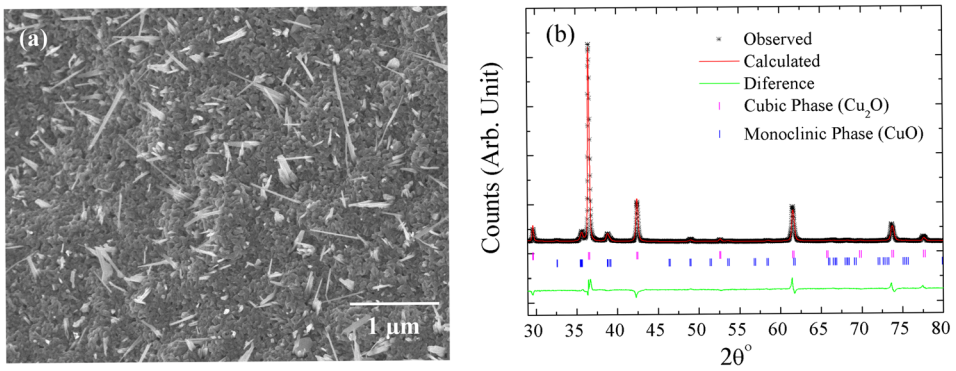

FIG. 1. (a) SEM micrograph and (b) Rietveld refinement of the XRD pattern of the nanostructured sample. Tick marks below the pattern indicate the expected Bragg reflection positions for cubic and monoclinic crystal phases.

The electrical current magnitude and exposed time play an important role regarding the morphology and number of nanowires.[9] Increasing the applied electrical current would result in an increase of the number of nanowires. A detailed synthesis study showing the role of current and time will be published elsewhere. Therefore, another sample was prepared in order to increase the number of nanowires, now by using an electrical current of 16 A. Fig. 2 shows the formation of CuO NWs on top of CuO NGs, both on top of a thick Cu_2O layer. The SEM images clearly show a very high density of well-defined CuO NWs growing from a thin layer of CuO nanograins on Cu_2O layer. The images also reveal that the CuO nanowires grow homogeneously on a ~170 nm layer of CuO nanograins on the top of Cu_2O layer. The mean diameter of the CuO nanowires is comprehended between 50 and 90 nm and the length up to 1.2 μm. The inset in Fig. 2(a) shows a TEM micrograph of an individual nanowire with its corresponding electron diffraction pattern. The nanowire is crystalline in nature, and its electron diffraction pattern was indexed as monoclinic with space group $C2/c$ near a $[0\bar{1}1]$ zone axis revealing that this nanostructure is the minority CuO phase in agreement with literature.[9] The CuO nanograins are close to 120 nm in diameter. The bulk Cu_2O layer has thickness of ~4.4 μm and a width of several micrometers. The XRD measurement along with Rietveld refinement indicated that the ratio of monoclinic CuO and cubic Cu_2O cubic phases has been increased significantly when compared to the first one. The analysis reveals 77% of Cu_2O and 23% of CuO, the cell parameters are: $a = 4.2529(1)$ and $V = 76.92(1)$ Å^3 for Cu_2O and $a = 4.664(2)$ Å, $b = 3.411(1)$ Å, $c = 5.115(2)$ Å, $\beta = 99.41(2)°$, and $V = 80.28(3)$ Å^3 for CuO. Energy dispersive spectroscopy (EDS) analyses further confirmed that the CuO and Cu_2O nanostructures are free of impurities (down to the detector sensitivity, i.e., 0.1 at. %).

A well established understanding of CuO NWs growth when using thermal oxidation process, which may be similar to resistive heating method, is that the formation of NWs from Cu metal oxidation requires a sequent growth of parallel oxide layers.[11] In this case, a Cu_2O layer is formed first followed by the formation of a CuO thin layer of NGs and

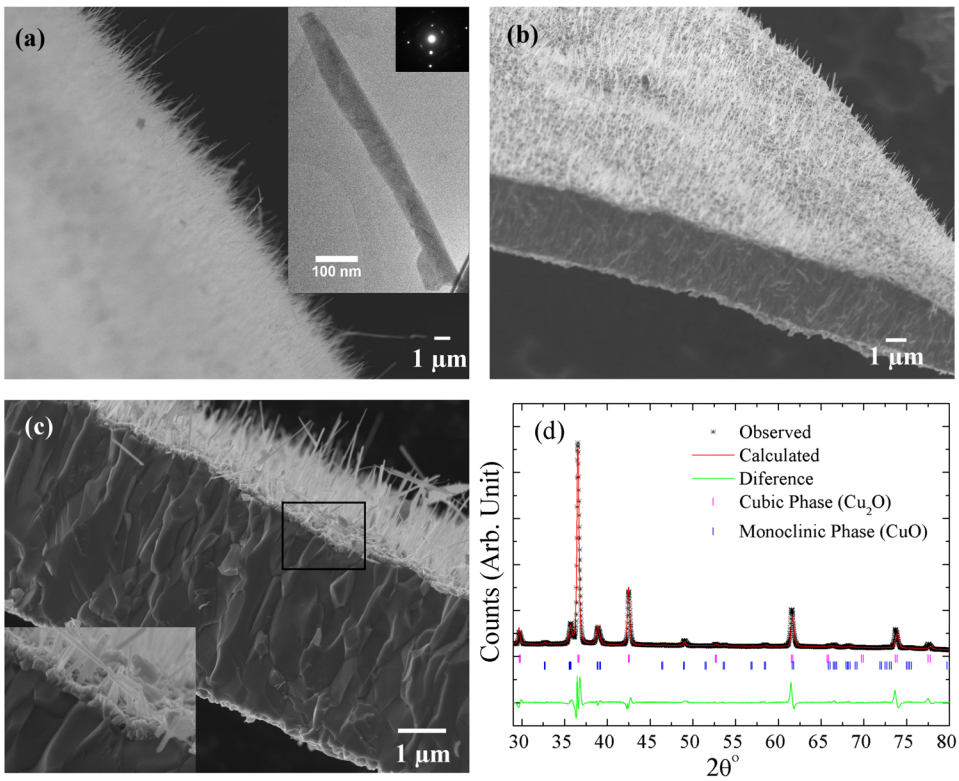

FIG. 2. (a)–(c) SEM images of the nanostructured sample with higher CuO/Cu_2O ratio. The inset of (a) shows a TEM image of a nanowire along with its electron diffraction pattern. The inset displays a thin layer of Cu O nanograins. (d) Rietveld refinement of the XRD pattern.

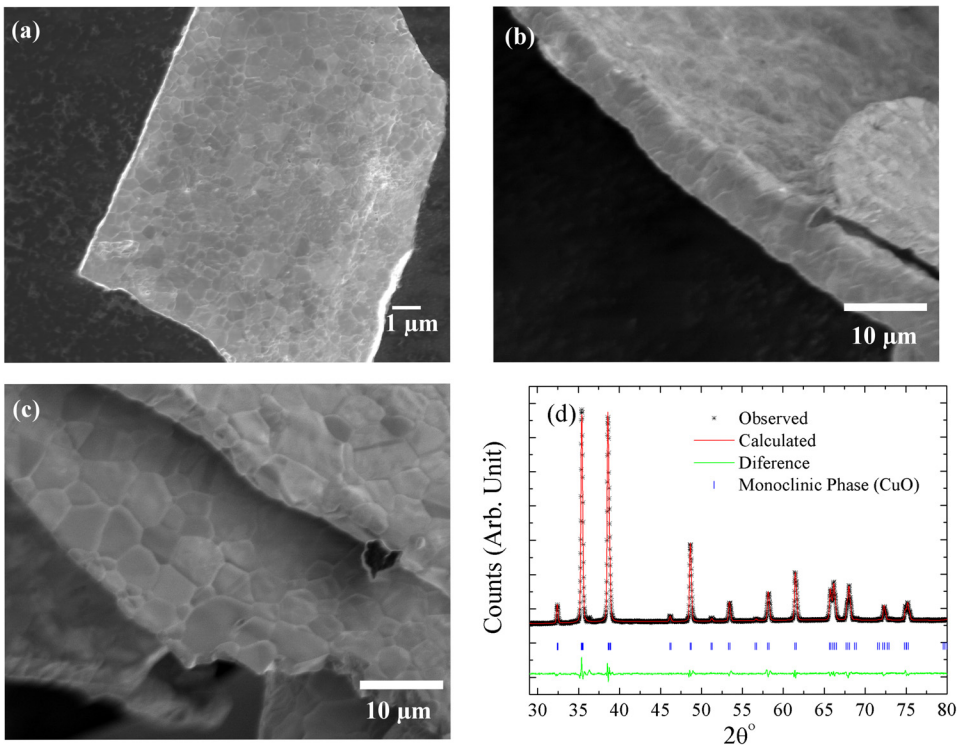

FIG. 3. (a)–(c) SEM micrographs and (d) XRD pattern with Rietveld refinement of the sample after a heat treatment at 900 °C.

subsequent growth of CuO NWs. CuO nanowires are then formed as a result of the competition between grain boundary and lattice diffusion of Cu ions across the Cu_2O layer.[12]

As we shall see, in order to interpret the magnetic susceptibility results it is important to characterize the same sample without nanograins/nanowires. Therefore, a heat treatment at high temperature (900 °C in air for 2 h) was performed in the sample after the magnetization measurements. Fig. 3 shows that layers with grains of few μm remain in the sample, but the nanowires and nanograins have completely disappeared. Surprisingly, XRD revealed that the cubic Cu_2O composition has turned into a bulk monoclinic CuO phase after the heat treatment. The cell parameters are $a = 4.6842(1)$ Å, $b = 3.4202(1)$ Å, $c = 5.1279(1)$ Å, $\beta = 99.44(1)°$, and $V = 81.04(1)$ Å^3.

CuO bulk samples has an unpaired electron in the *d*-shell exhibiting two AFM phase transitions—a commensurate collinear state at $T_N \sim 213$ K and an incommensurate spiral state at $T_N \sim 230$ K. On the other hand, Cu_2O has completely filled electronic *d*-shell leading to diamagnetic properties—the effective spin magnetic moment is zero. Magnetization measurements under zero field cooling (ZFC) and field cooling (FC) processes as a function of temperature with applied magnetic fields have been done on the three samples. First, we show in Fig. 4 results for the first sample which has less volume fraction of CuO phase and predominant presence of CuO nanograins. Fig. 4 indicates a linear change with temperature down to 50 K suggesting that the spins are freezed (Curie-like behavior is absent). The data also reveal the presence of a subtle kink in both ZFC and FC

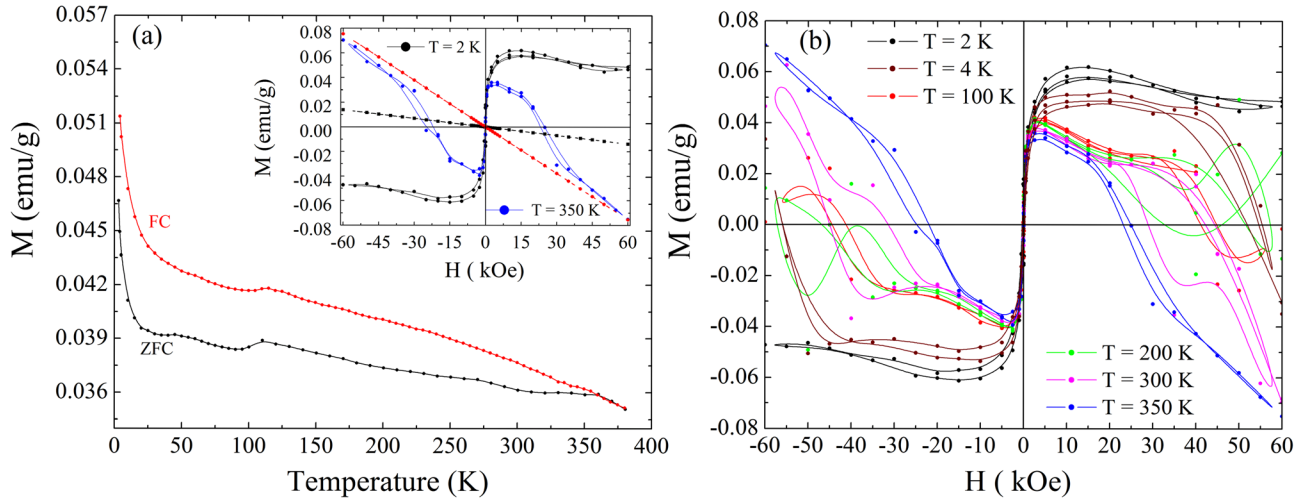

FIG. 4. (a) Magnetization measured at H = 5 kOe versus temperature for CuO nanograins on Cu_2O. The inset shows hysteresis measurement at two temperatures and diamagnetic contributions—the theoretically expected (black) and observed (red) taking into account the data at high magnetic field extrapolated to low field. (b) Magnetization versus magnetic field measured at different temperatures.

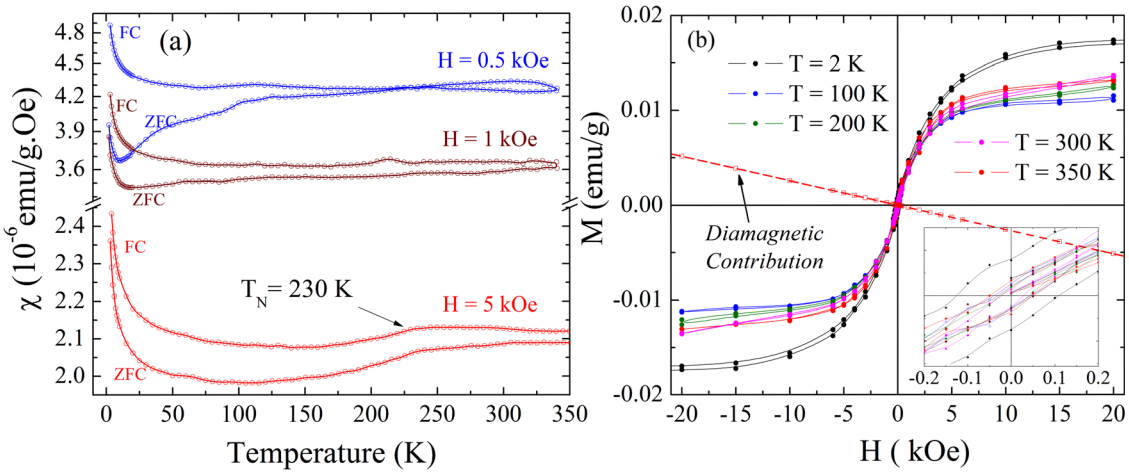

FIG. 5. (a) Magnetic susceptibility ($\chi = M/H$) measured at H = 0.5, 1, and 5 kOe for CuO nanowires/grains on the Cu_2O layer. (b) Magnetization as a function of magnetic field measured at different temperatures. The dashed line is the observed diamagnetic contribution. The inset shows an expanded view of the data at low magnetic field.

curves at $T_N = 110$ K which may suggest short range AFM order. Punnoose *et al.*[13] have suggested the presence of an antiferromagnetic transition at $T_N = 40$ K in CuO nanoparticles of 6.6 nm. The long-ranged magnetic order of spins may be inhibited due to the occurrence of broken magnetic bonds that change the total exchange energy. At low temperature around 20 K, the magnetization increases indicating a paramagnetic (PM)-like contribution.

The inset of Fig. 4 shows hysteresis loops measured at 2 K and 350 K. A ferromagnetic-like behavior is observed at both temperatures, the coercive field is 300 Oe and 40 Oe at T = 2 and T = 350 K, respectively. Even though this FM contribution is present at high temperatures, a superimposed negative contribution becomes dominant at T = 350 K. This diamagnetic temperature-independent contribution[26] comes from filled electronic *d*-shell of the Cu_2O layer in agreement with SEM and XRD results. The expected value of the diamagnetic contribution for our specimen can be calculated theoretically[14] which is 3.3×10^{-5} emu/mol Oe, as plotted in the inset of Fig. 4(a). At high magnetic fields, the diamagnetic contribution to the total magnetization becomes dominant; therefore, an experimental value can be estimated by extrapolating the magnetization at high fields to low fields. Interestingly, by doing this extrapolation we have obtained 1.8×10^{-4} emu/mol Oe (see inset of the Fig. 4(a)) which is one order of magnitude higher than that expected theoretically. In order to confirm this result, another nanostructured sample with lower amount of CuO on Cu_2O was measured and the observed value of the diamagnetic contribution was very close to the first measurement, 1.6×10^{-4} emu/mol. Oe. In Fig. 4(b), we show the hysteresis curves measured at several temperatures between 2 and 350 K. One can see that at high magnetic field and intermediate temperature the competition between FM from CuO nanostructures and diamagnetic from Cu_2O layer becomes severe, most pronounced above 20 kOe.

Fig. 5 displays the magnetic susceptibility as a function of temperature measured at three different magnetic fields for the sample with homogeneous dispersion of nanowires on the top of nanograins. The magnetization (ZFC and FC curves) measured at low magnetic field H = 0.5 kOe also reveals the absence of AFM ordering. It shows features that look like superparamagnetic behavior with irreversibility and a broad blocking temperature.[15] The magnetization measured at H = 1 kOe is nearly temperature independent down to 30 K. Interestingly, the antiferromagnetic phase transition expected in the bulk sample around T = 230 K shows up when measured at H = 5 kOe, as clearly seen in Fig. 5(a). This result reveals that the more homogeneous sample with nanowires of 50–90 nm in diameter on NGs shows long range order—characteristic of bulk properties.

We have performed hysteresis loop at several temperatures, displayed in Fig. 5(b), but only up to 20 kOe to prevent the induced competition between diamagnetic and ferromagnetic contributions. One can see a very distinct ferromagnetic-like behavior even below $T_N = 230$ K where the magnetic state is AFM as revealed by magnetization versus temperature measured at 5 kOe. However, at low field range, the magnetic moment increases and tends to saturate around 15 kOe. When the magnetic field is brought to zero a remanent magnetization with coercivity is observed, which is a signature of ferromagnetic behavior. As the ferromagnetic-like behavior is observed along with the AFM state, one could conclude the presence of an antiferromagnetically ordered core and a ferromagnetic-like contribution coming from uncompensated spins at the surface. Another possibility involving coexistence of AFM ordered region along with uncompensated spins region producing FM behavior would be the presence of defects throughout the sample. For example, lattice mismatch, crystalline boundary, and formation of a twin boundary along the longitudinal axis of the CuO nanowires.[27–29] Interestingly, the ferromagnetic-like behavior is observed even at 350 K, which is much higher temperature than the AFM transition at 230 K, suggesting that this behavior is not dependent on the original magnetic state of the sample, whether it is paramagnetic or AFM. It is interesting that Punnoose *et al.*[13] have shown that the magnetic behavior of particles with size greater than 10 nm already belongs to bulk properties with the absence of ferromagnetism. It is important to mention that the size reduction of bulk suppresses long range magnetic ordering due to

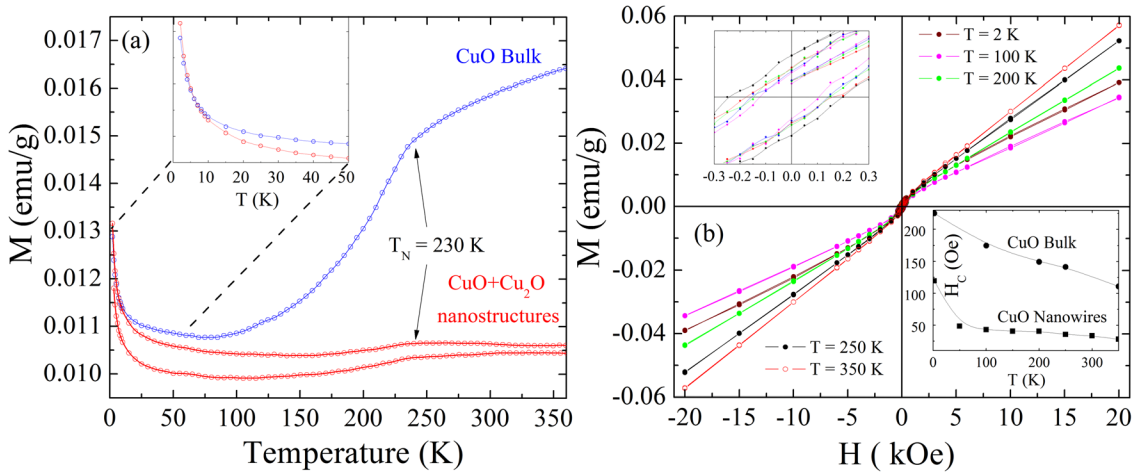

FIG. 6. (a) Magnetization as a function of temperature (FC) measured at H = 5 kOe for the sample after the heat treatment. The FC and ZFC measurements of CuO NWs on NGs + Cu_2O shown in Fig. 5(a) are plotted again for comparison. (b) Magnetization versus magnetic field measured at different temperatures for AFM CuO bulk sample. The upper inset shows an expanded view of the data at low magnetic field and the lower inset is the coercive field versus temperature for CuO bulk and CuO NWs/NGs.

finite size effect—the order parameter does not diverge due to domain or superparamagnetic limit. Therefore, at one hand, nanostructured materials shows ferromagnetism features and, at the other hand, there is a limit in size where molecular field breaks down inhibiting long range ferromagnetic ordering. Here, we observed enhanced FM features in samples with dimensions of 50–90 nm in diameter (~170 nm in thickness) and 1.2 μm in length. Another evident difference is the behavior of the magnetization versus magnetic field—the nanoparticles of 6.6 nm and 32 nm exhibit a linear dependence of the magnetization instead saturating when the magnetic field is increased.[13] Regarding other magnetic property studies in CuO, there is only a few works on nanostructured[16–18] samples which were prepared by different methods and most of them are concentrated on nanoparticles.[19–21] By doing a careful analysis of these published data, one realizes that a reasonable agreement among them is absent. This is evident from the behavior of the magnetization against temperature and magnetic field. We believe that these differences are very sensitive to shape, size of the nanostructure, and mainly to the synthesis preparation.

In Fig. 6, we show the magnetization measurements for the same sample, but after a heat treatment as characterized by SEM and XRD, shown in Fig. 3. The magnetic moment for CuO + Cu_2O nanostructures is lower than for CuO bulk which is in agreement with the fact that Cu_2O has a negative temperature-independent diamagnetic contribution. The antiferromagnetic phase transition is observed at $T_N = 230$ K. Above T_N, the magnetic susceptibility rises continuously due to one dimensional short range order.[22] Interestingly, this 1D short range order is suppressed in the nanostructured sample. At low temperature, the same robust paramagnetic-like behavior is observed in the bulk sample as observed in the nanostructured one. Since it is observed in the bulk sample, one can rule out size or surface effects due to nanometer scale which is usually suggested in the literature. This robust paramagnetic-like effect may be caused by the presence of few random isolated Cu^{+2} ions near the oxygen defects in the sample. A similar behavior is also observed in CoO nanoparticles[30] which also come from few isolated ions due to defects.

Fig. 6(b) displays the hysteresis loops measured at several temperatures revealing an antiferromagnetic behavior—the magnetization has linear dependence with magnetic field. It is important to reveal that even an AFM state shows hysteresis behavior with coercive field at low fields. The values of H_C for both samples are displayed in inset of Fig. 6(b). Interestingly, the coercive field value in the AFM bulk sample is higher than in the FM nanostructures. Vila *et al.*[23] have shown magnetic property measurements of CuO nanowires produced by thermal oxidation. The diameter of nanowires is in the range of 50–120 nm and lengths between 3 and 10 μm. The hysteresis behavior obtained by them (see Fig. 6 of Ref. 23) is very similar to the results of our bulk sample shown in Fig. 6(b). We believe that they observed only an AFM contribution in despite of the presence of a coercive field. It is important to emphasize that the presence of remanent magnetization and the coercive field is not enough to guarantee the presence of ferromagnetism coming from nanostructures which is usually suggested in the literature.

A careful inspection in Fig. 4(b) of the first nanostructured sample NGs reveals that the values of the saturation magnetic moment (M_{SAT}) is higher than that of the NWs on the top of NGs sample as shown in Fig. 5(b). Fig. 7(a) shows M_{SAT} for both samples as a function of temperature. For NGs sample, the higher value of M_{SAT} decreases monotonically as the temperature increases confirming the absence of long range magnetic ordering in this temperature interval. Therefore, as the spins are not aligned with each other a field-induced FM behavior will bring about a robust magnetic moment. On the other hand, the nanostructured sample that undergoes AFM phase transition displays a jump in M_{SAT} around 200 K when the system becomes paramagnetic revealing that part of the spins aligns and starts to contribute to the FM counterpart.

We have obtained the volume fraction of CuO phase on the top of Cu_2O layer to quantify the magnitude of the measured magnetic moment. For example, by using the SEM

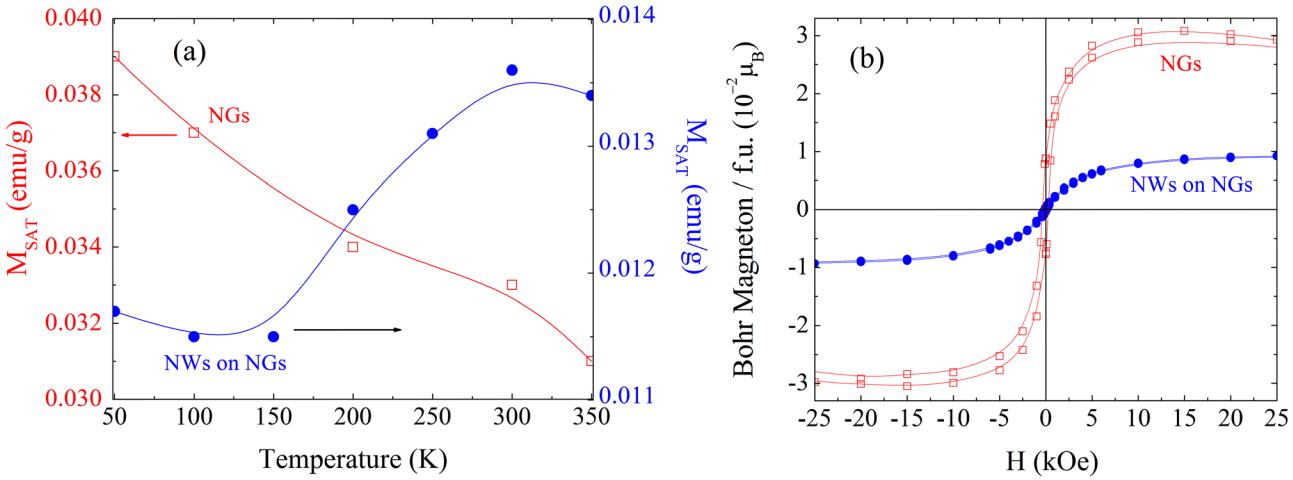

FIG. 7. (a) The saturation magnetization as a function of temperature for both CuO NGs and CuO NWs on NGs and (b) Bohr magneton versus magnetic field for the CuO NGs and CuO NWs on NGs.

images and the density of each crystal phase, we have found a relative mass of 5.7% of CuO and 94.3% of Cu_2O for NWs on the top of NGs sample and 3.0% of CuO and 97.0% of Cu_2O for NGs sample. Therefore, one can recalculate the value of magnetization measured at 2 K taking into account that all magnetic moment come from CuO. It is in agreement with the fact that Cu_2O is diamagnetic, which was subtracted. The magnetic moment in Bohr magneton unit per CuO formula is displayed in Fig. 7(b) for both samples. The magnetic-field-induced FM behavior for the sample with nanograins reaches $\sim 3 \times 10^{-2}$ μ_B/f.u. As one can see a value of $\sim 1 \times 10^{-2}$ μ_B/f.u. is obtained for the sample with nanowires on the top of nanograins. As the spins of ions in the ordered part of the nanostructure are antiparallel to each other, the magnetization will vanish, while at the surface and twinned boundary (and/or defects throughout the sample) spins are uncompensated resulting in a FM-like behavior. Straumal *et al.*[24] have shown that FM only appears if the ratio of grain-boundary area to grain volume (s_{GB}) exceeds a certain threshold value. Taking into account the dimensions of nanograins and nanowires of our samples, we have observed that ferromagnetism in nanograins should have the same magnitude as in nanowires. The magnetic moment measured by them in a set of ZnO thin film samples is in the range of 0.5 to 2×10^{-3} μ_B/f.u. Hong *et al.*[25] have also calculated the magnetic moment as a function of thickness for ZnO nanoplatelet and obtained values between 1 and 5×10^{-3} μ_B. Unfortunately, there is no theoretical calculation of FM contribution value when part of the sample is AFM ordered. We hope these experimental results will call attention of theoreticians.

In summary, we have produced CuO NGs and CuO NWs on the top of NGs samples by using electrical resistive heating method. The NGs sample shows absence of long range magnetic order and stronger field-induced FM behavior. In the sample comprised of NWs on NGs, the magnetization versus temperature (at low magnetic fields) resembles superparamagnetic behavior. However, a long range antiferromagnetic ordering is induced by a magnetic field of 5 kOe. A ferromagnetic-like contribution displaying remanent magnetization and coercivity was found to coexist in this system. Our results reveal clear experimental evidence that ferromagnetic-like behavior appears along with the presence of AFM ordering. The ferromagnetic-like behavior is also observed above the induced T_N, suggesting that this behavior is not dependent on the original magnetic state of system, whether it is PM or AFM. The effective magnetic moment was estimated to be 3×10^{-2} and 1×10^{-2} μ_B/f.u. for CuO NGs and CuO NWs on NGs, respectively.

This material is based upon work supported by the Brazilian agency CNPq under Grant Nos. 471863/2008-4, 485405/2011-3, and 305772/2011-2 and Fapesp under Grant Nos. 2009/18618-5, 2010/18364-0, and 2013/16172-5. We acknowledge the Brazilian Nanotechnology National Laboratory (LNNano), CNPEM, Campinas, Brazil for the TEM analyses (Process No. 14917).

[1]M. Law, L. E. Greene, J. C. Johnson, R. Saykally, and P. Yang, Nature Mater. **4**, 455 (2005); A. Wei, X. W. Sun, C. X. Xu, and Z. L. Dong, Appl. Phys. Lett. **88**, 213102 (2006); Y. Li, F. Qian, J. Xiang, and C. M. Lieber, Mater. Today **9**, 18 (2006).
[2]J. Osorio-Guillen, S. Lany, S. V. Barabash, and A. Zunger, Phys. Rev. Lett. **96**, 107203 (2006); Y. Belghazi, G. Schmerber, S. Colis, J. L. Rehspringer, A. Dinia, and A. Berrada, Appl. Phys. Lett. **89**, 122504 (2006); N. H. Hong, J. Sakai, and V. Brize, J. Phys.: Condens. Matter **19**, 036219 (2007); N. H. Hong, J. Sakai, N. Poirot, and V. Brizé, Phys. Rev. B **73**, 132404 (2006).
[3]M. Venkatesan, C. B. Fitzgerald, and J. M. D. Coey, Nature **430**, 630 (2004); M. D. Coey and S. A. Chambers, Mater. Res. Bull. **33**, 1053 (2008); D. W. Abraham, M. M. Frank, and S. Guha, Appl. Phys. Lett. **87**, 252502 (2005); M. S. Ramachandra Rao, D. C. Kundaliya, S. B. Ogale, L. F. Fu, S. J. Welz *et al.*, Appl. Phys. Lett. **88**, 142505 (2006); M. A. Garcia, E. Fernandez Pinel, J. de la Venta, A. Quesada, V. Bouzas *et al.*, J. Appl. Phys. **105**, 013925 (2009).
[4]A. Sundaresan, R. Bhargavi, N. Rangarajan, U. Siddesh, and C. N. R. Rao, Phys. Rev. B **74**, 161306 (2006).
[5]G. Zhu, H. Xu, Y. Xiao, Y. Liu, A. Yuan, and X. Shen, ACS Appl. Mater. Interfaces **4**, 744–751 (2012).
[6]T. Kimura, Y. Sekio, H. Nakamura, T. Siegrist, and A. P. Ramirez, Nature Mater. **7**, 291 (2008).
[7]D. P. Volanti, A. A. Felix, M. O. Orlandi, G. Whitfield, D.-J. Yang, E. Longo, H. L. Tuller, and J. A. Varela, Adv. Funct. Mater. **23**, 1759 (2013).
[8]M. Mashock, K. Yu, S. Cui, S. Mao, G. Lu, and J. Chen, ACS Appl. Mater. Interfaces **4**, 4192–4199 (2012).

[9]S. Rackauskas, A. G. Nasibulin, H. Jiang, Y. Tian, V. I. Kleshch, J. Sainio, E. D. Obraztsova, S. N. Bokova, A. N. Obraztsov, and E. I. Kauppinen, Nanotechnology **20**, 165603 (2009).
[10]B. J. Hansen, G. H. Lu, and J. H. Chen, J. Nanomater. **2008**, 830474.
[11]R. Memaa, L. Yuan, Q. Du, Y. Wang, and G. Zhou, Chem. Phys. Lett. **512**, 87–91 (2011).
[12]A. M. Goncalves, L. C. Campos, A. S. Ferlauto, and R. G. Lacerda, J. Appl. Phys. **106**, 034303 (2009).
[13]A. Punnoose, H. Magnone, M. S. Seehra, and J. Bonevich, Phys. Rev. B **64**, 174420 (2001).
[14]Landolt-Bornstein, in *New Series, Group II*, edited by K.-H. Hellwege and A. M. Hellwege (Springer-Verlag, Heidelberg, 1986), Vol. 16.
[15]M. Knobel, W. C. Nunes, L. M. Socolovsky, E. De Biasi, J. M. Vargas, and J. C. Denardin, J. Nanosci. Nanotechnol. **8**, 2836–2857 (2008).
[16]J. G. Zhaoa, S. J. Liub, S. H. Yanga, and S. G. Yang, Appl. Surf. Sci. **257**, 9678–9681 (2011).
[17]H.-M. Xiao, L.-P. Zhu, X.-M. Liu, and S.-Y. Fu, Solid State Commun. **141**, 431–435 (2007).
[18]S. R. Mishra, J. Losby, I. Dubenko, S. Roy, N. Ali, and K. Marasinghe, J. Magn. Magn. Mater. **279**, 111–117 (2004).
[19]A. E. Bianchi, S. J. Stewart, R. D. Zysler, and G. Punte, J. Appl. Phys. **112**, 083904 (2012).
[20]R. A. Borzi, S. J. Stewart, R. C. Mercader, G. Punte, and F. Garcia, J. Magn. Magn. Mater. **226–230**, 1513 (2001).
[21]G. N. Rao, Y. D. Yao, and J. W. Chen, IEEE Trans. Magn. **41**, 3409 (2005).
[22]M. O'Keeffe and F. S. Stone, J. Phys. Chem. Solids **23**, 261 (1962); O. Kondo, M. Ono, E. Sugiura, K. Sugiyama, and M. Date, J. Phys. Soc. Jpn. **57**, 3293 (1988).
[23]M. Vila, C. Díaz-Guerra, and J. Piqueras, J. Phys. D: Appl. Phys. **43**, 135403 (2010).
[24]B. B. Straumal, A. A. Mazilkin, S. G. Protasova, A. A. Myatiev, P. B. Straumal, G. Schütz, P. A. van Aken, E. Goering, and B. Baretzky, Phys. Rev. B **79**, 205206 (2009).
[25]J. I. Hong, J. Choi, S. S. Jang, J. Gu, Y. Chang, G. Wortman, R. L. Snyder, and Z. L. Wang, Nano Lett. **12**, 576–581 (2012).
[26]N. W. Ashcroftn and N. David Mermin, *Solid State Physics* (Cornell University, Saunders College Publishing, 1976).
[27]X. Jiang, T. Herricks, and Y. Xia, Nano Lett. **2**(12), 1333–1338 (2002).
[28]L. Yuan, Y. Wang, R. Mema, and G. Zhou, Acta Mater. **59**, 2491–2500 (2011).
[29]L. S. Huang, S. G. Yang, T. Li, B. X. Gu, Y. W. Du, Y. N. Lu, and S. Z. Shi, J. Cryst. Growth **260**, 130–135 (2004).
[30]D. Srikala, V. N. Singh, A. Banerjee, B. R. Mehta, and S. Patnaik, J. Phys. Chem. C **112**, 13882–13885 (2008).